IEEE Access
Multidisciplinary : Rapid Review : Open Access Journal

Received April 9, 2021, accepted April 22, 2021, date of publication April 27, 2021, date of current version May 5, 2021.

Digital Object Identifier 10.1109/ACCESS.2021.3075941

A GGIW-PHD Filter for Multiple Non-Ellipsoidal Extended Targets Tracking With Varying Number of Sub-Objects

YANG GONG[1], CHEN CUI[1], AND BIAO WU[2]
[1]Institute of Electronic Countermeasure, National University of Defense Technology, Hefei 230037, China
[2]Huayin Ordnance Test Center, Weinan 714000, China
Corresponding author: Yang Gong (gongyang17@nudt.edu.cn)

ABSTRACT When the extension state of the non-ellipsoidal extended target (NET) changes, the performance of traditional multiple target tracking algorithms based on the constant number of sub-objects will decrease. To solve this problem, this paper proposes a gamma Gaussian inverse Wishart probability hypothesis density filter for non-ellipsoidal extended targets with varying number of sub-objects, called VN-NET-GGIW-PHD filter. In the proposed filter, each NET is considered as a combination of multiple spatially close sub-objects, and the label management is introduced to realize the association between the NET and corresponding sub-objects. Then, by target spawning and combination, the number of sub-objects for approximating the extension state of each NET can be adjusted automatically. Furthermore, to obtain the partition of the measurement set, an approach based on the clustering by fast search and find of density peaks (CFSFDP) algorithm and expectation maximization (EM) algorithm is proposed. Simulation results show that the proposed filter can adaptively adjust the number of sub-objects and has better performance when the extension state of the NET changes.

INDEX TERMS Multi-target tracking, non-ellipsoidal extended target, target spawning, target combination, measurement set partition.

I. INTRODUCTION

In the traditional point target tracking algorithms, each target can at most generate one measurement per time step [1], [2]. With the resolution of modern sensors increasing, the target echo signal may be occupied in different range resolution cells. The sensor will receive multiple measurements from a target and the target is regarded as an extended target (ET) [3]. Recently, extended target tracking (ETT) has been hot research in target tracking field [4]–[6].

For extended target tracking, the spatial probability distribution is used to model the target extension state in [7]. The measurements of the target are assumed to be generated around the target and are Poisson distributed in number. Followed the model in [7], the extended target probability hypothesis density (ET-PHD) filter for multiple extended targets tracking is proposed by Mahler in [8]. The ET-PHD filter avoids the data association and reduces computational complexity. The extended target Gaussian Mixture PHD (ET-GM-PHD) filter in [9] and the extended target Particle PHD (ET-P-PHD) filter in [10] are proposed, which are suitable for linear Gaussian problems and nonlinear non-Gaussian systems, respectively. Furthermore, the cardinality-balanced multi-target multi-Bernoulli (CBMeMBer) filter [11] and the cardinalized PHD (CPHD) filter [12] for extended target tracking are proposed, respectively. Although the above filters can realize the multiple extended targets tracking, they cannot estimate the extension state of the target.

To estimate the extension state of extended target, the approach which models the extension state as a symmetric positive definite (SPD) random matrix is proposed by Koch in [13]. Based on this approach, the extension state is approximated by an ellipse. Considered the effect of true measurement noise, a modification of Koch's model is discussed in [14]. Granstrom [15] proposes a Gaussian inverse Wishart PHD (GIW-PHD) filter for multiple extended targets tracking where models the kinematic and extension states state as a Gaussian distribution and an inverse Wishart distribution, respectively. By modeling the measurement rate as

The associate editor coordinating the review of this manuscript and approving it for publication was Cesar Vargas-Rosales.

a Gamma distribution, a gamma GIW-PHD (GGIW-PHD) filter is further proposed by Granstrom in [16] to estimate the unknown measurement rate. The random matrix approach has been applied to many other filters in [17], [18]. However, these filters use only one ellipse to model the extension state and often lose information about size, shape and so on.

An approach which models the extension state of target by multiple sub-objects is proposed in [19]. The target is regarded as a non-ellipsoidal extended target (NET), and the target extension state is modeled by multiple ellipsoidal random matrices. But only a single extended target is considered without clutter in [19]. The multiple sub-objects approach has been further applied into PHD (called NET-GGIW-PHD) filter [20], CBMeMBer filter [21], GLMB filter [22] and realizes the multiple non-ellipsoidal extended targets tracking. However, it is assumed that sub-objects number for each NET remains constant during the whole process.

When the target attitude changes, the extension state of the target observed by sensors will change at the same time. For example, if the aircraft's attitude to the sensors changes from its belly to the head, the sensors can only observe the head instead of the wings and tail of the aircraft. If the number of sub-objects still remains constant, there will be a large estimate error on the extension state. In addition, for an aircraft carrier fleet, it can be regarded as a large NET. If the ships positions of the fleet change, the extension state of the aircraft carrier fleet may change at the same time. Using reasonable sub-objects number to approximate the extension state of the fleet may obtain more information about the fleet trend.

In [23], an algorithm for NET tracking with varying number of sub-objects is proposed, but it can only deal with one target scenario. In this work, a filter, called VN-NET-GGIW-PHD filter, is proposed with the varying number of sub-objects for multiple non-ellipsoidal extended targets tracking. The proposed filter consists of three aspects. Firstly, based on random matrix approach, each NET is regarded as a combination of multiple spatially close sub-objects, and the label management is introduced to realize the association between the NET and corresponding sub-objects. Then, target spawning and combination is utilized to adjust the sub-objects number for a NET automatically. Finally, an approach combined the clustering by fast search and find of density peaks (CFSFDP) algorithm with expectation maximization (EM) algorithm is proposed to partition the measurement set.

The remainder of this paper is organized as follows. In Section II, the models about ET and NET are discussed, and a brief introduction of NET-GGIW-PHD filter is given. The implementation of the proposed VN-NET-GGIW-PHD filter is given in Section III. The measurement set partition approach is presented in Section IV. The computational complexity analysis is given in Section V. Numerical simulations and conclusions are respectively presented in Section VI and Section VII.

II. BACKGROUND

A. ELLIPSOID EXTENDED TARGET MODEL

The set of extended targets is denoted by

$$\boldsymbol{\xi}_k = \left\{\boldsymbol{\xi}_k^{(i)}\right\}_{i=1}^{N_{x,k}}, \quad \boldsymbol{\xi}_k^{(i)} \triangleq \left(\gamma_k^{(i)}, \boldsymbol{x}_k^{(i)}, \boldsymbol{X}_k^{(i)}\right) \tag{1}$$

where k is the time step, $N_{x,k}$ is the number of extended targets, $\boldsymbol{\xi}_k^{(i)}$ is the state of ith extended target. $\gamma_k^{(i)}$ is the measurement rate that describes the average measurements number of ith target per time step. $\boldsymbol{x}_k^{(i)}$ and $\boldsymbol{X}_k^{(i)}$ are respectively the kinematic and extension states of ith extended target.

Assume $\gamma_k^{(i)}$ is independent of $\boldsymbol{x}_k^{(i)}$ and $\boldsymbol{X}_k^{(i)}$, and conditioned on the measurement set $\boldsymbol{Z}_k$, the target state $\boldsymbol{\xi}_k^{(i)}$ can be modeled as a GGIW distribution [16], [20]

$$\begin{aligned}
p\left(\boldsymbol{\xi}_k^{(i)} |\boldsymbol{Z}_k\right) &= p\left(\gamma_k^{(i)} |\boldsymbol{Z}_k\right) p\left(\boldsymbol{x}_k^{(i)} \middle|\boldsymbol{X}_k^{(i)}, \boldsymbol{Z}_k\right) p\left(\boldsymbol{X}_k^{(i)} |\boldsymbol{Z}_k\right)\\
&= \mathrm{G}(\gamma_k^{(i)}; \alpha_k^{(i)}, \beta_k^{(i)})\mathcal{N}(\boldsymbol{x}_k^{(i)}; \boldsymbol{m}_k^{(i)}, \boldsymbol{P}_k^{(i)} \otimes \boldsymbol{X}_k^{(i)})\\
&\quad \times \mathrm{IW}(\boldsymbol{X}_k^{(i)}; \upsilon_k^{(i)}, \boldsymbol{V}_k^{(i)})\\
&\triangleq GGIW(\boldsymbol{\xi}_k^{(i)}; \zeta_k^{(i)})
\end{aligned} \tag{2}$$

where $\mathrm{G}(\gamma; \alpha, \beta)$, $\mathcal{N}(x; m, P)$ and $\mathrm{IW}(X; \upsilon, V)$ denote the probability density function of gamma distribution, Gaussian distribution and inverse Wishart distribution, respectively. $\zeta_k^{(i)} = (\alpha_k^{(i)}, \beta_k^{(i)}, \boldsymbol{m}_k^{(i)}, \boldsymbol{P}_k^{(i)}, \upsilon_k^{(i)}, \boldsymbol{V}_k^{(i)})$ is the sufficient statistics of the ith GGIW component.

The target dynamic motion model is given by

$$\boldsymbol{x}_k^{(i)} = (\boldsymbol{F}_{k|k-1} \otimes \boldsymbol{I}_d)\boldsymbol{x}_{k-1}^{(i)} + \boldsymbol{w}_k^{(i)} \tag{3}$$

where $\boldsymbol{w}_k^{(i)}$ is Gaussian white noise with covariance $\boldsymbol{Q}_{k|k-1} \otimes \boldsymbol{X}_k^{(i)}$. $\boldsymbol{I}_d$ is an d dimension identity matrix where d is the dimension of the target extension state. $\otimes$ denotes the Kronecker product. The dimension of kinematic state is $n_x = s \times d$, where s is the length of kinematic state in one-dimensional space. Let $s = 3$, $\boldsymbol{F}_{k|k-1}$ and $\boldsymbol{Q}_{k|k-1}$ can be expressed as [15]

$$\boldsymbol{F}_{k|k-1} = \begin{bmatrix} 1 & \Delta & 0.5\Delta^2 \\ 0 & 1 & \Delta \\ 0 & 0 & e^{-\Delta/\theta} \end{bmatrix} \tag{4}$$

$$\boldsymbol{Q}_{k|k-1} = \sum^2 (1 - e^{-2\Delta/\theta})\mathrm{diag}([0, 0, 1]) \tag{5}$$

where Δ, $\sum$, and θ denote the sampling time, acceleration standard deviation and maneuver correlation time, respectively.

At time k, the measurement set is denoted as

$$\boldsymbol{Z}_k = \left\{z_k^{(j)}\right\}_{j=1}^{N_{Z,k}} \tag{6}$$

where $N_{z,k} = |\boldsymbol{Z}_k|$ is the number of measurements. The measurement model is given by

$$\boldsymbol{z}_k^{(j)} = (\boldsymbol{H}_k \otimes \boldsymbol{I}_d)\, \boldsymbol{x}_k^{(i)} + \boldsymbol{e}_k^{(j)} \tag{7}$$

$$\boldsymbol{e}_k^{(j)} \sim \mathcal{N}\left(\boldsymbol{e}_k^{(j)}, 0, \boldsymbol{B}_k^{(i)}\boldsymbol{X}_k^{(i)}(\boldsymbol{B}_k^{(i)})^T\right) \tag{8}$$

where $\boldsymbol{H}_k$= [100], $\boldsymbol{B}_k^{(i)} = (\rho\bar{\boldsymbol{X}}_{k|k-1}^{(i)} + \boldsymbol{R}_k)^{1/2}(\bar{\boldsymbol{X}}_{k|k-1}^{(i)})^{-1/2}$, $\bar{\boldsymbol{X}}_{k|k-1}^{(i)} = \boldsymbol{V}_{k|k-1}^{(i)}/(\upsilon_{k|k-1}^{(i)} - 2d - 2)$. ρ is used to describe the effect of $\boldsymbol{X}_k^{(i)}$ on the measurement noise. $\boldsymbol{R}_k$ denotes the true measurement noise covariance.

B. NON-ELLIPSOID EXTENDED TARGET MODEL

With the increase of sensor resolution, more detailed structure information about the target can be observed. Using only one ellipse to approximate the target extension state might lead to the loss of information, such as size, shape and orientation. In this case, the target is treated as a NET and can be approximated by multiple ellipses where each ellipse is regarded as a sub-object of the NET [19]. As shown in Fig. 1, more detailed information about target can be easily obtained by multiple ellipses.

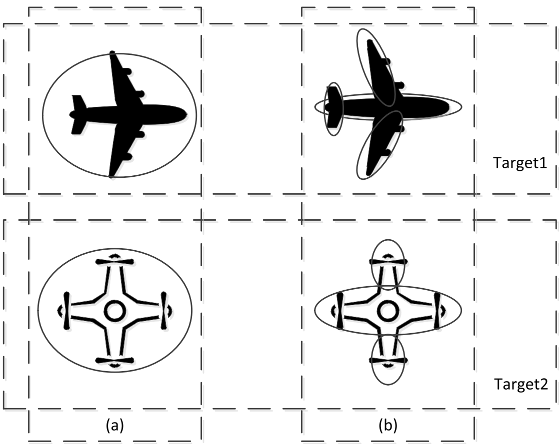

FIGURE 1. Illustration of non-ellipsoid extended targets approximated by one or multiple ellipses.

In this case, the set of non-ellipsoidal extended targets can be described as [20]

$$\boldsymbol{\xi}_k = \left\{ \left\{ \boldsymbol{\xi}_k^{(i,s)} \right\}_{s=1}^{n_k^{(i)}} \right\}_{i=1}^{N_{x,k}}, \quad \boldsymbol{\xi}_k^{(i,s)} \triangleq \left(\gamma_k^{(i,s)}, \boldsymbol{x}_k^{(i,s)}, \boldsymbol{X}_k^{(i,s)} \right) \tag{9}$$

where $n_k^{(i)}$ is the sub-objects number of ith NET, $\boldsymbol{x}_k^{(i,s)}$, $\gamma_k^{(i,s)}$,and $\boldsymbol{X}_k^{(i,s)}$ are kinematic state, measurement rate and extension state of sub-object s, respectively. Substituting (i) by (i, s) in (3) and (7), the dynamic motion model and measurement model of sub-object s can be obtained. The sub-object state $\boldsymbol{\xi}_k^{(i,s)}$ can be modeled as

$$\begin{aligned} p & \left(\boldsymbol{\xi}_k^{(i,s)} | \boldsymbol{Z}_k \right) \\ &= p \left(\gamma_k^{(i,s)} | \boldsymbol{Z}_k \right) p \left(\boldsymbol{x}_k^{(i,s)} \middle| \boldsymbol{X}_k^{(i,s)}, \boldsymbol{Z}_k \right) p \left(\boldsymbol{X}_k^{(i,s)} | \boldsymbol{Z}_k \right) \\ &= \mathrm{G}\gamma_k^{(i,s)}; \alpha_k^{(i,s)}, \beta_k^{(i,s)}) \mathcal{N}(\boldsymbol{x}_k^{(i,s)}; \boldsymbol{m}_k^{(i,s)}, \boldsymbol{M}_k^{(i,s)}) \\ & \quad \times \mathrm{IW}(\boldsymbol{X}_k^{(i,s)}; \upsilon_k^{(i,s)}, \boldsymbol{V}_k^{(i,s)}) \\ & \triangleq GGIW(\boldsymbol{\xi}_k^{(i,s)}; \zeta_k^{(i,s)}) \end{aligned} \tag{10}$$

where $\zeta_k^{(i,s)} = (\alpha_k^{(i,s)}, \beta_k^{(i,s)}, \boldsymbol{m}_k^{(i,s)}, \boldsymbol{P}_k^{(i,s)}, \upsilon_k^{(i,s)}, \boldsymbol{V}_k^{(i,s)})$ is the sufficient statistics, and $\boldsymbol{M}_k^{(i,s)} = \boldsymbol{P}_k^{(i,s)} \otimes \boldsymbol{X}_k^{(i,s)}$.

C. NET-GGIW-PHD FILTER

Based on the non-ellipsoidal extended target model, the NET-GGIW-PHD filter [20] is proposed to track multiple non-ellipsoidal extended targets. The NET-GGIW-PHD filter mainly consists of two parts, i.e., prediction and update. At time $k-1$, assume the multi-target posterior PHD can be denoted as

$$\begin{aligned} D_{k-1}(\boldsymbol{\xi}_{k-1}) &= \sum_{i=1}^{J_{k-1}} \sum_{s=1}^{n_k^{(i)}} \omega_{k-1}^{(i,s)} \mathrm{G}(\gamma_{k-1}; \alpha_{k-1}^{(i,s)}, \beta_{k-1}^{(i,s)}) \\ & \quad \times \mathcal{N}(\boldsymbol{x}_{k-1}; \boldsymbol{m}_{k-1}^{(i,s)}, \boldsymbol{P}_{k-1}^{(i,s)} \otimes \boldsymbol{X}_{k-1}) \\ & \quad \times \mathrm{IW}(\boldsymbol{X}_{k-1}; \upsilon_{k-1}^{(i,s)}, \boldsymbol{V}_{k-1}^{(i,s)}) \\ &= \sum_{i=1}^{J_{k-1}} \sum_{s=1}^{n_k^{(i)}} \omega_{k-1}^{(i,s)} GGIW(\boldsymbol{\xi}_{k-1}; \zeta_{k-1}^{(i,s)}) \end{aligned} \tag{11}$$

where J_{k-1} is the number of targets, and $\omega_{k-1}^{(i,s)}$ is the weight for sub-object s of ith target. The prediction of existing targets can be given by

$$\begin{aligned} & D_{k|k-1}^p(\boldsymbol{\xi}_k) \\ & \quad = \sum_{i=1}^{J_{k-1}} \sum_{s=1}^{n_k^{(i)}} \omega_{k|k-1}^{(i,s)} \mathrm{G}(\gamma_k; \alpha_{k|k-1}^{(i,s)}, \beta_{k|k-1}^{(i,s)}) \\ & \quad \quad \times \mathcal{N}(\boldsymbol{x}_k; \boldsymbol{m}_{k|k-1}^{(i,s)}, \boldsymbol{P}_{k|k-1}^{(i,s)} \otimes \boldsymbol{X}_k) \\ & \quad \quad \times \mathrm{IW}(\boldsymbol{X}_k; \upsilon_{k|k-1}^{(i,s)}, \boldsymbol{V}_{k|k-1}^{(i,s)}) \\ & \quad = \sum_{i=1}^{J_{k-1}} \sum_{s=1}^{n_k^{(i)}} \omega_{k|k-1}^{(i,s)} GGIW(\boldsymbol{\xi}_k; \zeta_{k|k-1}^{(i,s)}) \end{aligned} \tag{12}$$

where $\omega_{k|k-1}^{(i,s)} = p_{S,k} \omega_{k-1}^{(i,s)}$, $p_{S,k}$ is the probability of survival, and $\zeta_{k|k-1}^{(i,s)}$ is the predicted sufficient statistics.

The birth PHD is expressed as

$$D_k^b(\boldsymbol{\xi}_k) = \sum_{i=1}^{J_{b,k}} \sum_{s=1}^{n_k^{(i)}} \omega_{b,k}^{(i,s)} GGIW(\boldsymbol{\xi}_k; \zeta_{b,k}^{(i,s)}) \tag{13}$$

where $J_{b,k}$ is the number of new born targets, $\omega_{b,k}^{(i,s)}$ is the weight for sub-object s of ith new born target, and $\zeta_{b,k}^{(i,s)}$ is the corresponding sufficient statistics. The full predicted PHD can be denoted as

$$\begin{aligned} D_{k|k-1}(\boldsymbol{\xi}_k) &= D_{k|k-1}^p(\boldsymbol{\xi}_k) + D_k^b(\boldsymbol{\xi}_k) \\ &= \sum_{i=1}^{J_{k|k-1}} \sum_{s=1}^{n_k^{(i)}} \omega_{k|k-1}^{(i,s)} GGIW(\boldsymbol{\xi}_k; \zeta_{k|k-1}^{(i,s)}) \end{aligned} \tag{14}$$

where $J_{k|k-1} = J_{k-1} + J_{b,k}$. Then, the updated PHD can be expressed as

$$D_k(\boldsymbol{\xi}_k) = D_k^{ND}(\boldsymbol{\xi}_k) + \sum_{p \angle \boldsymbol{Z}_k} \sum_{W \in p} D_k^D(\boldsymbol{\xi}_k, W) \tag{15}$$

where $D_k^{ND}(\boldsymbol{\xi}_k)$ is the no detection part, and $D_k^D(\boldsymbol{\xi}_k, W)$ is the detection part. $p \angle \boldsymbol{Z}_k$ denotes the pth non-empty partition subset of $\boldsymbol{Z}_k$ and $W \in p$ denotes the Wth cell of the partition p.

Approximating the extension state of target by multiple ellipses, the NET-GGIW-PHD filter can realize the multiple non-ellipsoidal extended targets tracking. However, the

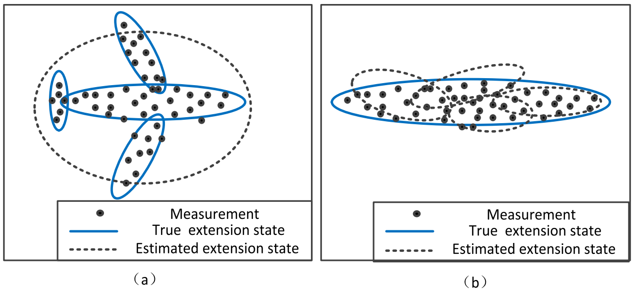

FIGURE 2. Illustration of extension state estimate for the NET.

number of sub-objects of each NET needs to be constant during the whole process. When the extension state of a NET changes during the tracking scenario, the method with constant number of sub-objects might not describe the extension state of the target well. Fig.2 gives an illustration of extension state estimate for the non-ellipsoidal extended target.

In Fig. 2(a), the true extension state is approximated by multiple ellipsoidal sub-objects. Many details will be ignored if the extension state is approximated by only one ellipse. By contrast, the multiple ellipsoidal sub-objects will occupy the area composed of only one sub-object in Fig. 2(b) and the extension state will be divided into multiple smaller parts. Therefore, there will be larger estimate error of extension state if the true number of the sub-ellipses is inconsistent with the estimated.

III. VN-NET-GGIW-PHD FILTER

In this section, we propose a VN-NET-GGIW-PHD filter, and the diagram of the filter is presented in Fig. 3. It mainly consists of target spawning, target combination, and measurement set partition.

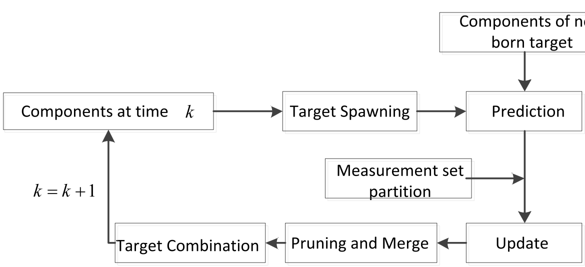

FIGURE 3. The diagram of the VN-NET-GGIW-PHD filter.

A. TARGET LABEL

It can be seen from Fig. 1 that the extension states of target 1 and 2 can be approximated by four and three ellipses, respectively. Therefore, the non-ellipsoidal extended targets 1 and 2 can be converted to four and three spatially close targets, respectively. Then, the multiple non-ellipsoidal extended targets can be regarded as multiple group targets where each of them consists of multiple spatially close ellipsoid extended sub-objects. In order to distinguish the different non-ellipsoidal extended targets, we introduce the target label management [24].

Based on the ellipsoid extended target model in section 2.1, we assign a unique label to each extended target, i.e., sub-object. Then, the set of multiple non-ellipsoidal extended targets can be denoted as

$$\boldsymbol{\xi}_k = \left\{\boldsymbol{\xi}_k^{(i)}\right\}_{i=1}^{N_{x,k}}, \quad \boldsymbol{\xi}_k^{(i)} \triangleq \left(\gamma_k^{(i)}, \boldsymbol{x}_k^{(i)}, X_k^{(i)}\right) \tag{16}$$

$$L_k = \left\{l_k^{(1)}, \ldots, l_k^{(N_{x,k})}\right\} \tag{17}$$

where $N_{x,k}$ is the number of ellipsoid sub-objects, and $l_k^{(i)}$ is the label of ith ellipsoid sub-object. Different from the non-ellipsoidal extended target model, the non-ellipsoidal extended target and sub-objects are associated by labels. The sub-objects belong to the same NET have the same labels, while the sub–objects belong to the different NET have the different labels. To realize the multi-target tracking, we have two assumptions as follows:

1) The type number of different non-ellipsoidal extended targets is known, represented by J;

2) The maximum number of sub-objects to approximate ith NET is known, represented by N_i. N_i is similar to $n_k^{(i)}$ in section 2.1.

Based on the above assumptions, the maximum sub-objects number for all non-ellipsoidal extended targets is calculated by $N_J^{\max} = \max\{N_1, \ldots, N_J\}$. For example, $J = 2, N_1 = 4$, $N_2 = 3$, and $N_J^{\max} = 4$ in Fig. 1. Combined with target label and ellipsoid extended target model, target spawning and combination are further introduced to deal with the number varying of sub-objects for NET tracking.

B. TARGET SPAWNING

When the true extension state of a NET cannot be approximated by one sub-object precisely, more additional sub-objects are needed to approximate the extension state. In this paper, we adopt the target spawning operation to add sub-objects. Similar to [25], the spawning event occurs in the prediction step. For all the sub-object components at time $k-1$, we choose the component $\boldsymbol{\xi}_{k-1}^{(i)}$ whose weight is greater than ω_{th} to perform spawning. Then, the spawning criterion can be shown as

$$\underbrace{\omega_{k-1}^{(i)} > \omega_{th}}_{\triangleq spa(\boldsymbol{\xi}_{k-1}^{(i)})} \tag{18}$$

where ω_{th} is the state extracted threshold. The corresponding label set is

$$L_{k,spa} = \left\{i = 1, \ldots, J_{k-1} \,\middle|\, \omega_{k-1}^{(i)} > \omega_{th}\right\} \tag{19}$$

Since there are multiple targets in the tracking scenario, the corresponding sub-objects number for each NET might be different. Due to less information about target spawning, it is difficult to determine the number of sub-objects for each NET. In order to avoid the extension state being not approximated properly after spawning, the maximum sub-objects number of each NET is utilized for spawning.

Given the target i which is satisfied with spawning criterion, the spawning sub-objects components are represented by

$$\begin{aligned}
&\sum_{r=1}^{J}\sum_{j=1}^{N_r}\sum_{l}^{d}\omega_{spa,k|k-1}^{(i,r,j,l)}GGIW(\boldsymbol{\xi}_k,\zeta_{spa,k|k-1}^{(i,r,j,l)})\\
&=\sum_{r=1}^{J}\sum_{j=1}^{N_r}\sum_{l=1}^{d}\omega_{spa,k|k-1}^{(i,r,j,l)}\mathrm{G}(\gamma_k;\alpha_{spa,k|k-1}^{(i,r,j,l)},\beta_{spa,k|k-1}^{(i,r,j,l)})\\
&\quad\times\mathcal{N}(\boldsymbol{x}_k;\boldsymbol{m}_{spa,k|k-1}^{(i,r,j,l)},\boldsymbol{P}_{spa,k|k-1}^{(i,r,j,l)}\otimes\boldsymbol{X}_k)\\
&\quad\times\mathrm{IW}(\boldsymbol{X}_k;\upsilon_{spa,k|k-1}^{(i,r,j,l)},\boldsymbol{V}_{spa,k|k-1}^{(i,r,j,l)}) \qquad (20)
\end{aligned}$$

$$l_{spa,k|k-1}^{(i,r,j,l)}=l_{k-1}^{(i)} \qquad (21)$$

$$\omega_{spa,k|k-1}^{(i,r,j,l)}=\omega_{k-1}^{(i)}/(dN_r) \qquad (22)$$

$$\alpha_{spa,k|k-1}^{(i,r,j,l)}=\alpha_{k-1}^{(i)} \qquad (23)$$

$$\beta_{spa,k|k-1}^{(i,r,j,l)}=\beta_{k-1}^{(i)}\cdot N_r \qquad (24)$$

$$\boldsymbol{P}_{spa,k|k-1}^{(i,r,j,l)}=\boldsymbol{P}_{k-1}^{(i)} \qquad (25)$$

$$\upsilon_{spa,k|k-1}^{(i,r,j,l)}=\upsilon_{k-1}^{(i)} \qquad (26)$$

$$\boldsymbol{V}_{spa,k|k-1}^{(i,r,j,l)}=\boldsymbol{V}_{k-1}^{(i)}/N_r \qquad (27)$$

If N_r is odd,

$$\boldsymbol{m}_{spa,k|k-1}^{(i,r,j,l)}=\boldsymbol{m}_{k-1}^{(i)}+((N_r+1)/2-j)\sqrt{\boldsymbol{e}_l^{(i)}}\boldsymbol{H}^T v_l^{(i)} \qquad (28)$$

If N_r is even,

$$\boldsymbol{m}_{spa,k|k-1}^{(i,r,j,l)}=\begin{cases}\boldsymbol{m}_{k-1}^{(i)}+((N_r+2)/2-j)\sqrt{\boldsymbol{e}_l^{(i)}}\boldsymbol{H}^T\mathbf{v}_l^{(i)} & j\le N_r/2\\ \boldsymbol{m}_{k-1}^{(i)}+(N_r/2-j)\sqrt{\boldsymbol{e}_l^{(i)}}\boldsymbol{H}^T\mathbf{v}_l^{(i)} & j>N_r/2\end{cases} \qquad (29)$$

$\boldsymbol{e}_l^{(i)}$ is the eigenvalue of $\bar{\boldsymbol{X}}_{k-1|k-1}^{(i)}$ and $\mathbf{v}_l^{(i)}$ is the corresponding eigenvector. Then, all the spawning sub-objects PHD and labels set can be denoted by

$$\begin{aligned}
&D_k^{spa}(\boldsymbol{\xi}_k)\\
&=\sum_{i=1}^{L_{k,spa}}\sum_{r=1}^{J}\sum_{j=1}^{N_r}\sum_{l}^{d}\omega_{spa,k|k-1}^{(i,r,j,l)}GGIW(\boldsymbol{\xi}_k,\zeta_{spa,k|k-1}^{(i,r,j,l)})\\
&=\sum_{i=1}^{L_{k,spa}}\sum_{r=1}^{J}\sum_{j=1}^{N_r}\sum_{l=1}^{d}\omega_{spa,k|k-1}^{(i,r,j,l)}\mathrm{G}(\gamma_k;\alpha_{spa,k|k-1}^{(i,r,j,l)},\beta_{spa,k|k-1}^{(i,r,j,l)})\\
&\quad\times\mathcal{N}(\boldsymbol{x}_k;\boldsymbol{m}_{spa,k|k-1}^{(i,r,j,l)},\boldsymbol{P}_{spa,k|k-1}^{(i,r,j,l)}\otimes\boldsymbol{X}_k)\\
&\quad\times\mathrm{IW}(\boldsymbol{X}_k;\upsilon_{spa,k|k-1}^{(i,r,j,l)},\boldsymbol{V}_{spa,k|k-1}^{(i,r,j,l)}) \qquad (30)
\end{aligned}$$

$$\begin{aligned}
&L_{k,spa}\\
&=\left\{\left\{\left\{\left\{l_{spa,k|k-1}^{(i,r,j,l)}\right\}_{l=1}^{d}\right\}_{j=1}^{N_r}\right\}_{r=1}^{J}\right\}_{i=1}^{L_{k,spa}} \qquad (31)
\end{aligned}$$

C. TARGET COMBINATION

When one sub-object is enough to approximate the true extension state of the target, multiple sub-objects should be combined. Target combination is performed after the PHD update. For the two sub-objects $\boldsymbol{\xi}_{k-1}^{(i)}$ and $\boldsymbol{\xi}_k^{(j)}$ with weight greater than ω_{th}, they should be combined if they are spatially close, have the same label and similar velocity, namely

$$S_{over}/\min(S_i,S_j)<u_{over} \qquad (32)$$

$$\left|\mathrm{v}_k^{(i)}-\mathrm{v}_k^{(j)}\right|<u_{\mathrm{v}} \qquad (33)$$

$$l_k^{(i)}=l_k^{(j)} \qquad (34)$$

where S_{over} is the overlap area of two sub-objects' extension states. S_i and S_j are the areas of two sub-objects' extension states, $\mathrm{v}_k^{(i)}$ and $\mathrm{v}_k^{(j)}$ are corresponding velocity vectors. u_{over} and u_{v} are the thresholds for area and velocity, respectively. Then, the combination criterion can be expressed as

$$\underbrace{\begin{matrix}\frac{S_{over}}{\min(S_i,S_j)}<u_{over}\&\left|\mathrm{v}_k^{(i)}-\mathrm{v}_k^{(j)}\right|<u_{\mathrm{v}}\\ \&l_k^{(i)}=l_k^{(j)}\&(\omega_k^{(i)}>\omega_{th}\&\omega_k^{(j)}>\omega_{th})\end{matrix}}_{\triangleq Comb(\boldsymbol{\xi}_k^{(i)},\boldsymbol{\xi}_k^{(j)})} \qquad (35)$$

Given sub-object i and sub-object j which are satisfied with combination criterion, the GGIW parameters of combination target component can be represented as

$$l_{comb,k}=l_k^{(i)}=l_k^{(j)} \qquad (36)$$

$$\omega_{comb,k}=\frac{\alpha_k^{(i)}}{\alpha_k^{(i)}+\alpha_k^{(j)}}\omega_k^{(i)}+\frac{\alpha_k^{(j)}}{\alpha_k^{(i)}+\alpha_k^{(j)}}\omega_k^{(j)} \qquad (37)$$

$$\alpha_{comb,k|k}=\alpha_k^{(i)}+\alpha_k^{(j)} \qquad (38)$$

$$\beta_{comb,k|k}=(\beta_k^{(i)}+\beta_k^{(j)})/2 \qquad (39)$$

$$\boldsymbol{m}_{comb,k|k}=\frac{\alpha_k^{(i)}}{\alpha_k^{(i)}+\alpha_k^{(j)}}\boldsymbol{m}_k^{(i)}+\frac{\alpha_k^{(j)}}{\alpha_k^{(i)}+\alpha_k^{(j)}}\boldsymbol{m}_k^{(j)} \qquad (40)$$

$$\boldsymbol{P}_{comb,k|k}=\frac{\alpha_k^{(i)}}{\alpha_k^{(i)}+\alpha_k^{(j)}}\boldsymbol{P}_k^{(i)}+\frac{\alpha_k^{(j)}}{\alpha_k^{(i)}+\alpha_k^{(j)}}\boldsymbol{P}_k^{(j)} \qquad (41)$$

$$\upsilon_{comb,k|k}=\frac{\alpha_k^{(i)}}{\alpha_k^{(i)}+\alpha_k^{(j)}}\upsilon_k^{(i)}+\frac{\alpha_k^{(j)}}{\alpha_k^{(i)}+\alpha_k^{(j)}}\upsilon_k^{(j)} \qquad (42)$$

$$\boldsymbol{V}_{comb,k|k}=\frac{\alpha_k^{(i)}}{\alpha_k^{(i)}+\alpha_k^{(j)}}\boldsymbol{V}_k^{(i)}+\frac{\alpha_k^{(j)}}{\alpha_k^{(i)}+\alpha_k^{(j)}}\boldsymbol{V}_k^{(j)} \qquad (43)$$

After the combination, delete the GGIW components of sub-object i and sub-object j and add the combination component into the update PHD.

Remark: If there are multiple sub-objects satisfying the combination criterion, two components with the largest weight are combined. After the combination, the original two components are deleted and the combination component is extracted. Then the remaining components are performed by combination criterion and hypothesis continuously.

D. THE IMPLEEMENTATION OF VN-NET-GGIW-PHD FILTER

This subsection will give the detailed implementation of VN-NET-GGIW-PHD filter. At time $k-1$, suppose the multi-target posterior PHD can be approximated by a mixture of GGIW components denoted by

$$\begin{aligned} D_{k-1}(\boldsymbol{\xi}_{k-1}) &= \sum\nolimits_{i=1}^{J_{k-1}} \omega_{k-1}^{(i)} GGIW(\boldsymbol{\xi}_{k-1}, \zeta_{k-1}^{(i)}) \\ &= \sum\nolimits_{i=1}^{J_{k-1}} \omega_{k-1}^{(i)} \mathrm{G}(\gamma_{k-1}; \alpha_{k-1}^{(i)}, \beta_{k-1}^{(i)}) \\ &\quad \times \mathcal{N}(\boldsymbol{x}_{k-1}; \boldsymbol{m}_{k-1}^{(i)}, \boldsymbol{P}_{k-1}^{(i)} \otimes \boldsymbol{X}_{k-1}) \\ &\quad \times \mathrm{IW}(\boldsymbol{X}_{k-1}; \upsilon_{k-1}^{(i)}, \boldsymbol{V}_{k-1}^{(i)}) \end{aligned} \tag{44}$$

$$L_{k-1} = \left\{ l_{k-1}^{(1)}, l_{k-1}^{(2)}, \ldots, l_{k-1}^{(J_{k-1})} \right\} \tag{45}$$

where $\omega_{k-1}^{(i)}$ is the weight of ith component, L_{k-1} is the corresponding labels set. The predicted PHD and label set of existing targets can be denoted by

$$\begin{aligned} D_{k|k-1}^{p}(\boldsymbol{\xi}_k) &= \sum\nolimits_{i=1}^{J_{k-1}} \omega_{k|k-1}^{(i)} \mathrm{G}(\gamma_k; \alpha_{k|k-1}^{(i)}, \beta_{k|k-1}^{(i)}) \\ &\quad \times \mathcal{N}(\boldsymbol{x}_k; \boldsymbol{m}_{k|k-1}^{(i)}, \boldsymbol{P}_{k|k-1}^{(i)} \otimes \boldsymbol{X}_k) \\ &\quad \times \mathrm{IW}(\boldsymbol{X}_k; \upsilon_{k|k-1}^{(i)}, \boldsymbol{V}_{k|k-1}^{(i)}) \end{aligned} \tag{46}$$

$$L_{k|k-1}^{p} = \left\{ l_{k-1}^{(1)}, l_{k-1}^{(2)}, \ldots, l_{k-1}^{(J_{k-1})} \right\} \tag{47}$$

where $\omega_{k|k-1}^{(i)} = p_S \omega_{k-1}^{(i)}$. The birth PHD and labels set are denoted by

$$\begin{aligned} D_k^{b}(\boldsymbol{\xi}_k) &= \sum\nolimits_{i=1}^{J_{b,k}} \omega_{b,k}^{(i)} \mathrm{G}(\gamma_k; \alpha_{b,k}^{(i)}, \beta_{b,k}^{(i)}) \\ &\quad \times \mathcal{N}(\boldsymbol{x}_k; \boldsymbol{m}_{b,k}^{(i)}, \boldsymbol{P}_{b,k}^{(i)} \otimes \boldsymbol{X}_k) \\ &\quad \times \mathrm{IW}(\boldsymbol{X}_k; \upsilon_{b,k}^{(i)}, \boldsymbol{V}_{b,k}^{(i)}) \end{aligned} \tag{48}$$

$$L_{b,k} = \left\{ l_{b,k}^{(1)}, \ldots, l_{b,k}^{(J_{b,k})} \right\} \tag{49}$$

where $\omega_{b,k}^{(i)}$ is the weight of ith new born target, $J_{b,k}$ is the new born targets number, $l_{b,k}^{(i)}$ is the label of ith new born target, $\zeta_{b,k}^{(i)} = (\alpha_{b,k}^{(i)}, \beta_{b,k}^{(i)}, \boldsymbol{m}_{b,k}^{(i)}, \boldsymbol{P}_{b,k}^{(i)}, \upsilon_{b,k}^{(i)}, \boldsymbol{V}_{b,k}^{(i)})$ is the corresponding sufficient statistics. The spawning PHD and labels set are given in (30-31), and then the full predicted PHD and labels set can be denoted as

$$\begin{aligned} D_{k|k-1}(\boldsymbol{\xi}_k) &= D_{k|k-1}^{p}(\boldsymbol{\xi}_k) + D_k^{b}(\boldsymbol{\xi}_k) + D_k^{spa}(\boldsymbol{\xi}_k) \\ &= \sum\nolimits_{i=1}^{J_{k|k-1}} \omega_{k|k-1}^{(i)} GGIW(\boldsymbol{\xi}_k, \zeta_{k|k-1}^{(i)}) \end{aligned} \tag{50}$$

$$L_{k|k-1} = L_{k|k-1}^{p} \cup L_{b,k} \cup L_{k,spa} \tag{51}$$

The updated PHD at time k is given by

$$D_k(\boldsymbol{\xi}_k) = D_k^{ND}(\boldsymbol{\xi}_k) + \sum_{p\angle \boldsymbol{Z}_k} \sum_{W\in p} D_k^{D}(\boldsymbol{\xi}_k, W) \tag{52}$$

And the corresponding labels set is

$$L_k = L_k^{ND} + \sum_{p\angle \boldsymbol{Z}_k} \sum_{W\in p} L_k^{D}(\boldsymbol{\xi}_k, W) \tag{53}$$

The parameters and labels set of no detection part $D_k^{ND}(\boldsymbol{\xi}_k)$ is given by

$$\begin{aligned} D_k^{ND}(\boldsymbol{\xi}_k) &= \sum_{i=1}^{J_{k|k-1}} (1-p_{D,k})\omega_{k|k-1}^{(i)} GGIW(\boldsymbol{\xi}_k, \zeta_{k|k}^{(i)}) \\ &\quad + \sum_{i=1}^{J_{k|k-1}} p_{D,k}\omega_{k|k-1}^{(i)} \left(\frac{\beta_{k|k-1}^{(i)}}{\beta_{k|k-1}^{(i)}+1} \right)^{\alpha_{k|k-1}^{(i)}} \\ &\quad \times GGIW(\boldsymbol{\xi}_k, \bar{\zeta}_{k|k}^{(i)}) \end{aligned} \tag{54}$$

$$\begin{aligned} \bar{\zeta}_{k|k}^{(i)} &= (\alpha_{k|k-1}^{(i)}, \beta_{k|k-1}^{(i)}+1, \boldsymbol{m}_{k|k-1}^{(i)}, \boldsymbol{P}_{k|k-1}^{(i)}, \\ &\quad \times \upsilon_{k|k-1}^{(i)}, \boldsymbol{V}_{k|k-1}^{(i)}) \end{aligned} \tag{55}$$

$$\zeta_{k|k}^{(i)} = \zeta_{k|k-1}^{(i)} \tag{56}$$

$$L_k^{ND} = L_{k|k-1} \tag{57}$$

where $p_{D,k}$ is the detection probability. The detection part $D_k^{D}(\boldsymbol{\xi}_k, W)$ calculates the product of the likelihood of the measurements in each cell and the predicted GGIW components given by

$$\begin{aligned} D_k^{D}(\boldsymbol{\xi}_k, W) &= \sum_{i=1}^{J_{k|k-1}} (\lambda c_k(z_k))^{-|W|} \mathcal{L}_k^{(i,W)} \\ &\quad \times \mathrm{G}(\gamma_k; \alpha_k^{(i,W)}, \beta_k^{(i,W)}) \\ &\quad \times \mathcal{N}(\boldsymbol{x}_k; \boldsymbol{m}_k^{(i,W)}, \boldsymbol{P}_k^{(i,W)} \otimes \boldsymbol{X}_k) \\ &\quad \times \mathrm{IW}(\boldsymbol{X}_k; \upsilon_k^{(i,W)}, \boldsymbol{V}_k^{(i,W)}) \end{aligned} \tag{58}$$

where λ is the average clutter number, $c_k(z_k)$ is the spatial distribution of the clutter. For details about parameters and weights of GGIW components, please refer to [15], [20]. In addition, the corresponding labels set is

$$L_k^{D}(\boldsymbol{\xi}_k, W) = L_{k|k-1} \tag{59}$$

Then the pruning and merging of GGIW components is performed similar to [21] and the posterior PHD and labels set are expressed as

$$\begin{aligned} D_k(\boldsymbol{\xi}_k) &= \sum_{j=1}^{J_k} \omega_k^{(i)} \mathrm{G}(\gamma_k; \alpha_k^{(i)}, \beta_k^{(i)}) \mathrm{IW}(\boldsymbol{X}_k; \upsilon_k^{(i)}, \boldsymbol{V}_k^{(i)}) \\ &\quad \times \mathcal{N}(\boldsymbol{x}_k; \boldsymbol{m}_k^{(i)}, \boldsymbol{P}_k^{(i)} \otimes \boldsymbol{X}_k) \\ &= \sum_{j=1}^{J_k} \omega_k^{(i)} GGIW(\boldsymbol{\xi}_k, \zeta_k^{(i)}) \end{aligned} \tag{60}$$

$$L_k = \left\{ l_k^{(1)}, \ldots, l_k^{(J_k)} \right\} \tag{61}$$

where J_k is the number of components after pruning and merging. Perform the target combination, and the multi-target posterior PHD and labels set are given by

$$D_k(\boldsymbol{\xi}_k) = \sum\nolimits_{i=1}^{\tilde{J}_k} \omega_k^{(i)} GGIW(\boldsymbol{\xi}_k, \tilde{\zeta}_k^{(i)}) \tag{62}$$

$$L_k = \left\{ l_k^{(1)}, \ldots, l_k^{(\tilde{J}_k)} \right\} \tag{63}$$

where $\tilde{J}_k$ is the number of components after target combination, $\tilde{\xi}_k^{(i)}$ is the corresponding sufficient statistics.

The estimate of sub-object states, labels set and the number of non-ellipsoidal extended targets are given by

$$\hat{\boldsymbol{\xi}}_k = \left\{ \boldsymbol{\xi}_k^{(i)} \middle| \omega_k^{(i)} > \omega_{th}, i = 1, \ldots \tilde{J}_k \right\} \tag{64}$$

$$\hat{L}_k = \left\{ l_k^{(i)} \middle| \omega_k^{(i)} > \omega_{th}, i = 1, \ldots \tilde{J}_k \right\} \tag{65}$$

$$\hat{N} = \text{unique}(\hat{L}_k) \tag{66}$$

where unique(x) denotes the number of elements that are not repeated in x.

IV. PARTITION OF THE MEASUREMENT SET

The key to multiple extended target tracking is the measurement set partition. Several partitioning methods, such as distance partition [9] and prediction partition [15] have been proposed to partition the measurement set. Since distance partitioning relies on the distance thresholds, it burdens with high computation complexity with the increase of measurements number. Besides, since the measurements generated from the same NET are spatially close, distance partition cannot deal with the NET tracking well. Although the sub-partitioning methods [9], [26] can be used to solve the above problem to some extent, they often fail when the sub-objects have different sizes. Prediction partition uses the predicted positions of targets to partition the measurement set. It is sensitive to maneuver and is not suitable for the scenario where the sub-objects number for the NET varies during the tracking process.

In this section, we propose a measurement set partition method. The proposed partition method consists of two stages. At the first stage, the CFSFDP algorithm [27] is introduced to partition the measurement set into multiple groups and remove the clutter. The measurements in each group are generated from the same NET. At the second stage, the EM algorithm is used to partition the measurements in each group into multiple clusters where the measurements in each cluster are regarded from the same sub-object.

A. PARTITIONING THE MEASUREMENT SET INTO GROUPS BY CFSFDP ALGORITHM

As a clustering algorithm, the CFSFDP algorithm needs neither the prior information of cluster number nor iteration and it can realize clustering rapidly. CFSFDP algorithm calculates the local density ρ_i of each data point and its distance δ_i from points with higher density. The ρ_i and δ_i can be expressed as

$$\rho_i = \sum_j \mathrm{X}(d_{ij} - d_c) \tag{67}$$

$$\delta_i = \begin{cases} \min(d_{ij}) & \text{if } \rho_j > \rho_i \\ \max(d_{ij}) & \text{others} \end{cases} \tag{68}$$

where d_c is the cutoff distance, and d_{ij} is the distance between data point i and data point j. $\mathrm{X}(x) = 1$ if $x \leq 0$ and $\mathrm{X}(x) = 0$ otherwise. In CFSFDP algorithm, the cluster centers usually have a higher local density and a relatively large distance from other point with higher local density. The outliers have a lower local density and a relatively large distance from other point with higher local density. Then, the cluster centers can be found and outliers will be removed. Each remaining point will be clustered to its nearest neighbor center with higher density.

In our paper, the CFSFDP algorithm is used to partition the measurement set $\mathbf{Z}_k$. If $\rho_i \geq \rho_c$ and $\delta_i \geq \delta_c$, $\boldsymbol{z}_k^i$ is the cluster center. If $\rho_i < \rho_c$ and $\delta_i \geq \delta_c$, $\boldsymbol{z}_k^i$ is the clutter. ρ_c and δ_c are the density threshold and distance threshold, respectively. After the cluster centers are determined, the clutter can be removed and the remaining measurements will be clustered.

B. PARTITIONING THE GROUPS BY EM ALGORITHM

Since the sub-objects belonging to the same NET are close to each other, the CFSFDP algorithm can only partition the measurement set into groups where the measurements in each group are generated from the same NET. In order to evaluate the extension state of NET sufficiently, the groups need to be partitioned further, called sub-partitioning. Essentially, sub-partitioning is also a clustering problem. Considered the measurements generated from sub-objects follow the Gaussian distribution, the Gaussian mixture model (GMM) [28] can be used to model the measurements in each group. The parameters of each Gaussian model consist of weight, mean and covariance, represented by $\boldsymbol{\theta} = \left\{\pi_l, \boldsymbol{\mu}_l, \sum_l\right\}_{l=1}^{N_{sub}}$. π_l, $\boldsymbol{\mu}_l$ and $\sum_l$ are the weight, mean and covariance parameters of lth sub-object, N_{sub} is the number of sub-objects. As for a clustering algorithm, EM algorithm has been widely used for GMM in [15], [28], [29]. Therefore, we partition the groups by EM algorithm in this paper.

The EM algorithm can proceed iteratively until convergence if the number of GMM is known. However, sub-objects number for each NET is unknown and varying. In order to cover all the cases where the sub-objects number varies, $N_{sub} = 1, \ldots, N_J^{\max}$ is adopted for each group. In addition, the performance of EM algorithm depends highly on the initial cluster centers. The EM algorithm might converge to the local optimal if the initial centers are inappropriate. To solve this problem, multiple hypotheses method is utilized for initialization as Table 1.

In Table 1, $\mathbf{Z}_k^s = \left\{z_k^1, \ldots, z_k^m\right\}$ is the measurement set of sth group, m is the corresponding number of measurements, and M_h is the number of initial hypotheses. It can be seen from table 1 that each group is initialized by $N_J^{\max} M_h$ parameters, and $N_J^{\max} M_h$ partitions will be obtained by EM algorithm. Since the same partitions may be obtained by different initial parameters, the repeated partitions will be deleted after sub-partitioning of each group. The total partition of the measurement set can be obtained after all the groups are partitioned and integrated.

Remark: Several model selection methods such as Bayesian information criterion [30], minimum message length (MML) criterion [31], and Akaike's information

TABLE 1. Parameter initialization of EM algorithm.

Input: $\boldsymbol{Z}_k^s=\left\{z_k^1,\ldots,z_k^m\right\}$, M_h, N_{sub}
Define: $z_c=\frac{1}{m}\sum_{i=1}^m \boldsymbol{z}_k^{(i)}$, $r_z=\frac{1}{2}\max_i \left\Vert \boldsymbol{z}_k^i-\boldsymbol{z}_c\right\Vert_2$ for $h=1:M_h$ for $l=1:N_{sub}$ $\pi_l^h=\frac{1}{N_{sub}}$, $\Sigma_l^h=\frac{1}{10d}\mathrm{tr}\left(\frac{1}{m}\sum_{i=1}^m(\boldsymbol{z}_k^{(i)}-\boldsymbol{z}_c)(\boldsymbol{z}_k^{(i)}-\boldsymbol{z}_c)^T\right)\boldsymbol{I}_d$ $\boldsymbol{\mu}_l^h=\begin{cases}\boldsymbol{z}_c+r_z\begin{bmatrix}\cos\left(\frac{2\pi(l-2)}{N_{sub}-1}+\frac{2\pi(h-1)}{N_{sub}M_h}\right)\\ \sin\left(\frac{2\pi(l-2)}{N_{sub}-1}+\frac{2\pi(h-1)}{N_{sub}M_h}\right)\end{bmatrix} & N_{sub}>1\\ \boldsymbol{z}_c & N_{sub}=1\end{cases}$ end end
Output: $\boldsymbol{\theta}=\left\{\left\{\pi_l^h,\boldsymbol{\mu}_l^h,\Sigma_l^h\right\}_{l=1}^{N_{sub}}\right\}_{h=1}^{M_h}$

criterion (AIC) criterion [32] can be utilized to obtain the sub-objects number estimate for each group. However, due to the measurement uncertainty, the estimate of sub-objects number may be biased, which will lead to the underestimate or overestimate of sub-objects number after PHD update. Therefore, in this paper, $N_{sub}=1,\ldots,N_J^{\max}$ is chosen to initialize the GMM.

Then, the proposed VN-NET-GGIW-PHD filter can be summarized in Table 2.

TABLE 2. The proposed VN-NET-GGIW-PHD filter.

Input: $\xi_{k-1}=\left\{\xi_{k-1}^{(i)}\right\}_{i=1}^{J_{k-1}}$, $\omega_{k-1}^{(i)}$, $L_{k-1}=\left\{l_{k-1}^{(1)},l_{k-1}^{(2)},\ldots,l_{k-1}^{(J_{k-1})}\right\}$, $\zeta_{k-1}^{(i)}=(\alpha_{k-1}^{(i)},\beta_{k-1}^{(i)},\boldsymbol{m}_{k-1}^{(i)},\boldsymbol{P}_{k-1}^{(i)},\upsilon_{k-1}^{(i)},\boldsymbol{V}_{k-1}^{(i)})$, $\boldsymbol{Z}_{k-1}$
Step1:Perform target spawning by Equation (18-31); **Step2**:Prediction Compute the quantities of the predicted PHD by Equation (50-51); **Step3**: Partition the measurement set $\boldsymbol{Z}_{k-1}$ by CFSFDP algorithm and EM algorithm; **Step4**: Update Compute the quantities of the updated PHD by Equation (52-59); **Step5**: Pruning and merge; **Step6**: Perform state extraction by Equation (64-66);
Output: $\xi_k=\left\{\xi_k^{(i)}\right\}_{i=1}^{J_k}$, $\omega_k^{(i)}$, $L_k=\left\{l_k^{(1)},l_k^{(2)},\ldots,l_k^{(J_k)}\right\}$, $\zeta_k^{(i)}=(\alpha_k^{(i)},\beta_k^{(i)},\boldsymbol{m}_k^{(i)},\boldsymbol{P}_k^{(i)},\upsilon_k^{(i)},\boldsymbol{V}_k^{(i)})$

V. COMPUTATIONAL COMPLEXITY ANALYSIS

In general, the computational complexity of the proposed algorithm consists of two parts: the computational complexity of partitioning the measurement set and the computational complexity of PHD update. Although we add the label management, target spawning and target combination, the computational complexity of them can be ignored compared with partitioning the measurement set and PHD update.

A. THE COMPUTATIONAL COMPLEXITY OF PARTITIONING THE MEASUREMENT SET

For the GGIW-PHD filter, the distance partition [9] is used to partition the measurement set. The computational complexity of distance partition in the worst case is approximated as $O(N_{z,k}^4)$ [33]. $N_{z,k}$ is the number of measurements. In our manuscript, the CFSFDP algorithm is used to partition the measurement set into multiple groups and then each group is partitioned by the EM algorithm. The computational complexity of CFSFDP algorithm is approximated as $O(N_{z,k}^2)$. Besides, the EM algorithm is used for sub-partitioning, and its computational complexity can be approximated as $O(\tau N M_h m^2)$. Where τ is the average iteration number, N is the number of groups, m is the corresponding number of measurements in each group and M_h is the number of initial hypotheses. Compared with distance partition, the proposed algorithm has much less computational complexity when $N_{z,k}$ is larger. For the NET-GGIW-PHD filter, it uses the prediction partition [15] to partition the measurement set. However, it cannot deal with the case where the sub-objects number changes with the extension state. In our simulation, the proposed partition method is used for NET-GGIW-PHD filter.

B. THE COMPUTATIONAL COMPLEXITY OF PHD UPDATE

As for the computational complexity of PHD update, the computational complexity of all three filters is approximated as $O(n_x^2 J_{k|k-1}\sum_{i=1}^{P}|p_i|)$. n_x is the dimension of the target state vector P is the partition number and $J_{k|k-1}$ is the number of predicted Gaussian components. The partition number of the proposed partition algorithm is much fewer than that of distance partition. And for the proposed partition algorithm, the clutter is eliminated and $|p_i|$ in each partition is much fewer than that of distance partition. Its computational complexity is much lower than that of distance partition.

VI. SIMULATION RESULTS

To demonstrate the performance of the proposed VN-NET-GGIW-PHD filter, we take NET-GGIW-PHD filter [20] and GGIW-PHD filter [16] as comparisons. For each simulation, 50 Monte Carlo trials are performed. The target number, sub-objects number and a variant of optimal sub-pattern assignment (OSPA) distance [17] are used as the metric. Assume the true set of sub-objects is

$$\xi_k=\left\{\xi_k^{(i)}\right\}_{i=1}^{N_{x,k}},\quad \xi_k^{(i)}\triangleq\left(\gamma_k^{(i)},\boldsymbol{x}_k^{(i)},\boldsymbol{X}_k^{(i)}\right) \tag{69}$$

The estimated set of sub-objects is

$$\hat{\boldsymbol{\xi}}_k = \left\{\hat{\boldsymbol{\xi}}_k^{(i)}\right\}_{i=1}^{\hat{N}_{x,k}}, \quad \hat{\boldsymbol{\xi}}_k^{(i)} \triangleq \left(\hat{\gamma}_k^{(i)}, \hat{\boldsymbol{x}}_k^{(i)}, \hat{\boldsymbol{X}}_k^{(i)}\right) \tag{70}$$

The distance between $\boldsymbol{\xi}_k^{(i)}$ and $\hat{\boldsymbol{\xi}}_k^{(j)}$ can be expressed as

$$d(\boldsymbol{\xi}_k^{(i)}, \hat{\boldsymbol{\xi}}_k^{(j)}) = \frac{w_\gamma}{c_\gamma} d_{i,j}^{(c_\gamma)} + \frac{w_x}{c_x} d_{i,j}^{(c_\gamma)} + \frac{w_X}{c_X} d_{i,j}^{(c_X)} \tag{71}$$

where $w_\gamma + w_x + w_X = 1$, and

$$\begin{cases} d_{i,j}^{(c_\gamma)} = \min(c_\gamma, \left|\gamma_k^{(i)} - \hat{\gamma}_k^{(j)}\right|) \\ d_{i,j}^{(c_x)} = \min(c_x, \left\|\boldsymbol{x}_k^{(i)} - \hat{\boldsymbol{x}}_k^{(j)}\right\|_2) \\ d_{i,j}^{(c_X)} = \min(c_X, \left\|\boldsymbol{X}_k^{(i)} - \hat{\boldsymbol{X}}_k^{(j)}\right\|_F) \end{cases} \tag{72}$$

where $|\cdot|$, $\|\cdot\|_2$ and $\|\cdot\|_F$ are the absolute value, Euclidean norm and the Frobenius norm, respectively. The constants c_γ, c_x and c_X are the maximum expected error of the measurement rate, kinematic state and extension state, respectively.

If $N_{x,k} \leq \hat{N}_{x,k}$, the variant of OSPA distance is given by

$$d_p^{(c)}(\boldsymbol{\xi}_k, \hat{\boldsymbol{\xi}}_k) = \left(\frac{1}{\hat{N}_{x,k}}\left(\sum_{i=1}^{N_{x,k}}\left(d_{i,\pi(i)}^{c}\right)^p + c^p(\hat{N}_{x,k} - N_{x,k})\right)\right)^{1/p} \tag{73}$$

where $d_{i,j}^{(c)} = \min(c, d(\boldsymbol{\xi}_k^{(i)}, \hat{\boldsymbol{\xi}}_k^{(j)})), \pi = \underset{\pi \in \Pi_{\hat{N}_{x,k}}}{\arg\min} \sum_{i=1}^{N_{x,k}} (d_{i,j}^{(c)})^p$. If $N_{x,k} > \hat{N}_{x,k}$, the OSPA distance is given by $d_p^{(c)}(\hat{\boldsymbol{\xi}}_k, \boldsymbol{\xi}_k)$.

The sampling period is $\Delta = 1$ s, acceleration standard deviation is $\theta = 1$ s, and maneuver correlation time is $\sum = 0.1$ m/s^2. The true measurement noise covariance $\boldsymbol{R}_k = \mathrm{diag}([1, 1])$ and $\rho = 1$. The expected number of measurements generated by each sub-object is Poisson distribution. The survival probability of target is $p_{S,k} = 0.99$, the detection probability is $p_{D,k} = 0.98$. The clutter is uniformly distributed over the surveillance region and the average clutter number is $\lambda = 10$. The OSPA parameters are $p = 1, c_\gamma = 10, c_x = 30, c_X = 300, c = 0.7$, $w_\gamma = 0.1, w_x = 0.6$, and $w_X = 0.3$. The new born components parameters are $\omega_{k,b}^{(i)} = 0.1, \boldsymbol{m}_{b,k}^{(i)} = [(\boldsymbol{x}_0^{(i)})^T \boldsymbol{0}_4^T], \boldsymbol{P}_{k,b}^{(i)} = \mathrm{diag}([100^2, 25^2, 25^2]), \upsilon_{b,k}^{(i)} = 10$, $\boldsymbol{V}_{b,k}^{(i)} = \mathrm{diag}([1, 1]), \alpha_{b,k}^{(i)} = 20, \beta_{b,k}^{(i)} = 1$, and $L_{b,k} = \left\{l_{b,k}^{(1)}, \ldots, l_{b,k}^{(J_{b,k})}\right\}$. The mean vector $\boldsymbol{m}_{b,k}^{(i)}$ is the starting position of non-ellipsoidal extended target. For pruning and merging, $T' = 10^{-3}, \mathbb{S}' = 0.6$ and $J_{\max} = 100$. The state extracted threshold is $\omega_{th} = 0.5$, area threshold is $u_{over} = 0.3$, and velocity threshold is $u_v = 50$. For the partition of the measurement set, $\delta_c = d_c = 60, \rho_c = 2, M_h = 4$. Since the prediction partition method in [20] cannot deal with the case where the sub-objects number changes with the extension state, the measurement set is partitioned by the proposed partition algorithm for NET-GGIW-PHD filter, where $N_{sub} \in \{N_1, \ldots, N_J^{\max}\}$.

Two simplified non-ellipsoidal extended targets (T1 and T2) with different sub-objects number are shown in Fig. 4. Target T1 is composed of three sub-objects and target T2 is composed of two sub-objects.

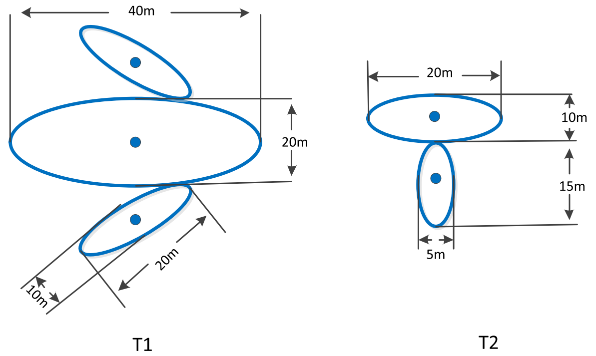

FIGURE 4. Illustration of target T1 and T2.

A. ONE TARGET SCENARIO

In this scenario, only one non-ellipsoidal extended target T1 is considered. The surveillance region is $[-1500, 1500]$ m $\times$ $[-1000, 1000]$ m and the total time is 100 s. Target T1 appears at time $k = 1$ and is composed of three sub-objects at the beginning. From time $k = 1$ to $k = 35$, T1 moves with a constant velocity. At time $k = 36$, T1 begins to turn with a constant turn rate $-\pi/30$ and continues to time $k = 65$. During the turn, T1 consists of only one sub-object because of the change of attitude. At time $k = 66$, T1 reverts to a non-ellipsoidal extended target with three sub-objects and moves to time $k = 100$ with constant velocity. If T1 is composed of three sub-objects, the expected measurements numbers of sub-objects are 20, 15, and 15, respectively. If T1 is composed of only one sub-object, the expected measurements number of sub-object is 20. The target trajectory and measurements are shown in Fig. 5.

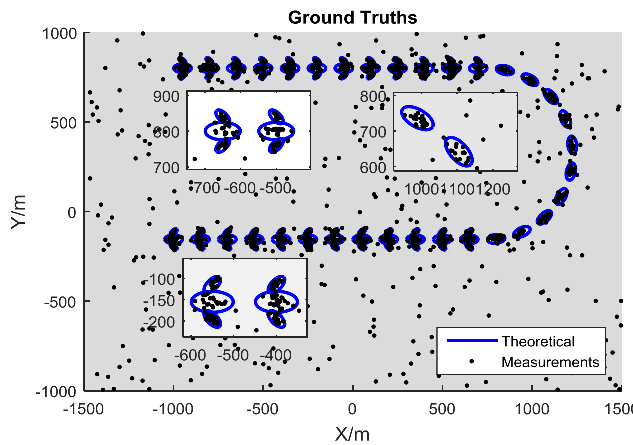

FIGURE 5. Target trajectory and measurements.

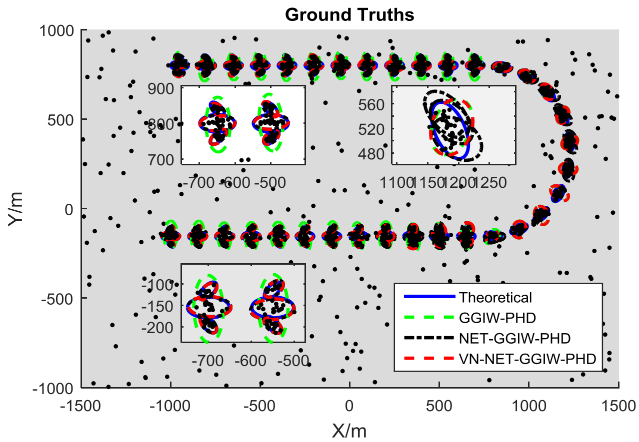

FIGURE 6. The simulation results in one trial.

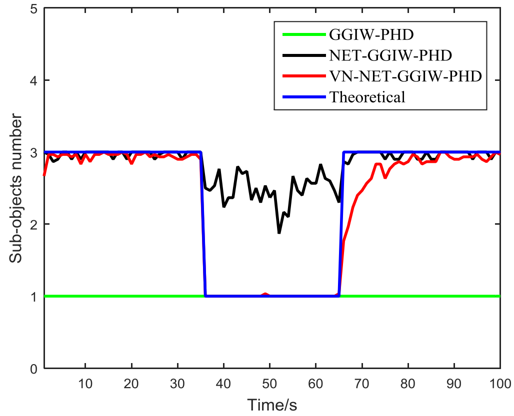

FIGURE 8. The estimate of sub-objects number.

The filters output of a single trial is shown in Fig.6. We can notice that the GGIW-PHD filter approximates the extension state by an ellipse during the whole process. When the true sub-objects number is equal to three, the GGIW-PHD filter will wrongly estimate one target with the larger extension state. When the true sub-objects number is equal to one, the extension state can be estimated accurately. By contrast, the NET-GGIW-PHD filter has the opposite characteristic. Compared with the above filters, the VN-NET-GGIW-PHD filter can approximate the extension state with the appropriate number of sub-objects during the whole process no matter where the target extension state is changed or not.

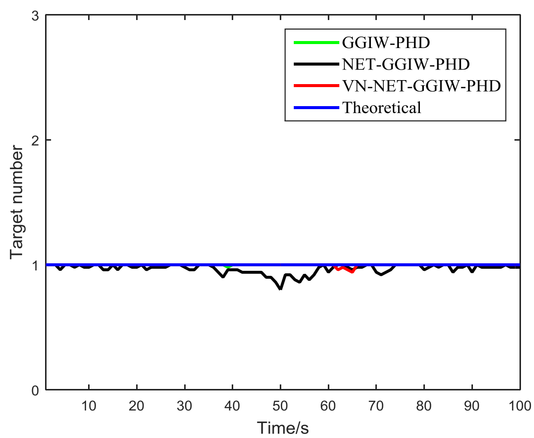

FIGURE 7. The estimate of target number.

Fig. 7 and Fig. 8 show the estimate of target number and sub-objects number by 50 Monte Carlo trials. It can be seen that all three filters can produce an unbiased estimate of target number. Since the assumed sub-objects number in NET-GGIW-PHD filter is not consistent with the truth when target turns, the target may be missing after PHD update. It leads to the slight underestimate of target number for NET-GGIW-PHD filter. In Fig.7, the estimated sub-objects number is equal to the target number for GGIW-PHD filter. This is because the GGIW-PHD filter models the extension state by only an ellipse. The estimate of sub-objects number for NET-GGIW-PHD filter has high accuracy during the most time except for the case where the target turns. Through the target spawning and combination, the VN-NET-GGIW-PHD filter can adaptively adjust the sub-objects number to approximate the extension state and has the best estimate accuracy of sub-objects number.

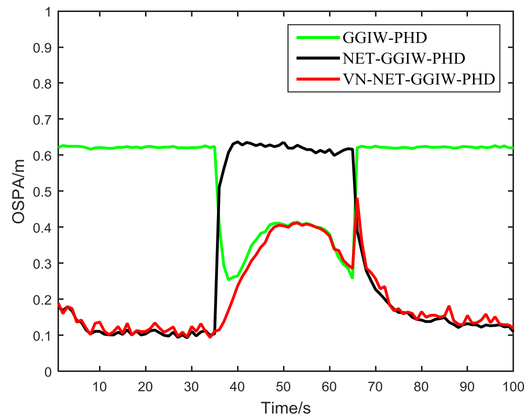

FIGURE 9. The estimate of sub-objects number.

Fig. 9 shows the OSPA distance of three filters by 50 Monte Carlo trials. The GGIW-PHD filter has low OSPA distance only when one sub-object exists. On the contrary, the NET-GGIW-PHD has low OSPA distance when three sub-objects exist. Compared with the GGIW-PHD filter and NET-GGIW-PHD filter, the VN-NET-GGIW-PHD filter has the lowest OSPA distance during the whole process. However, when the target turns, the target extension state's estimate error will increase, which leads to slight increase of OSPA distance.

Fig. 10 gives the average run time of each step for GGIW-PHD filter and VN-NET-GGIW-PHD filter by 50 Carlo trials. It can be seen that the average run time of the proposed filter is much less than the GGIW-PHD filter. This is because the number of partitions for distance partition will increase due to more distance thresholds, which lead to higher

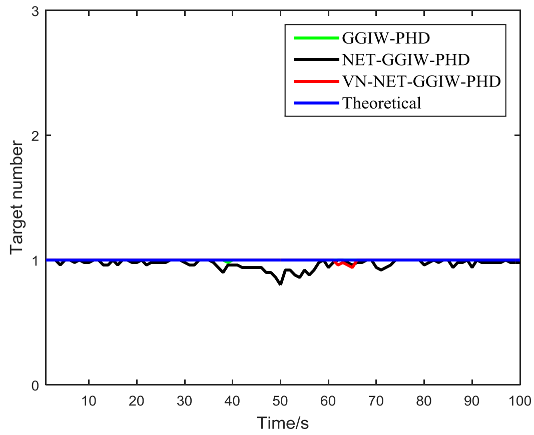

FIGURE 10. Average run time of each step.

computation. In contrast, the proposed filter adopt CFSFDP algorithm and EM algorithm to partition the measurement set, which can reduce the computation sharply.

B. MULTIPLE TARGETS SCENARIO

Two non-ellipsoidal extended targets (T1 and T2) are considered in this scenario. The surveillance region is $[-1000, 4000]$ m $\times$ $[-1000, 2000]$ m and the total time is 100 s. Two targets move along with the constant velocity. Target T1, consisting of three sub-objects, appears at time $k = 1$. The extension state of T1 changes at time $k = 31$ and consists of only one sub-object. At time $k = 61$, T1 reverts to consisting of three sub-objects and continues to time $k = 100$. The expected measurements numbers of sub-objects are same as that in Section VI-A. Target T2, consisting of two sub-objects, appears at time $k = 10$ and disappears at time $k = 80$. The true measurement rates of T2 are both 15. The target trajectory and measurements are shown in Fig. 11.

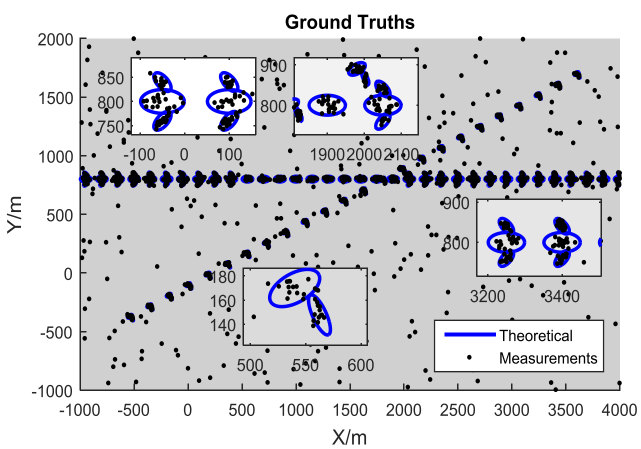

FIGURE 11. Target trajectory and measurements.

Fig. 12 gives the filters output in one trial. It can be seen that the VN-NET-GGIW-PHD filter can estimate the kinematic and extension states accurately. Fig. 13 and Fig. 14

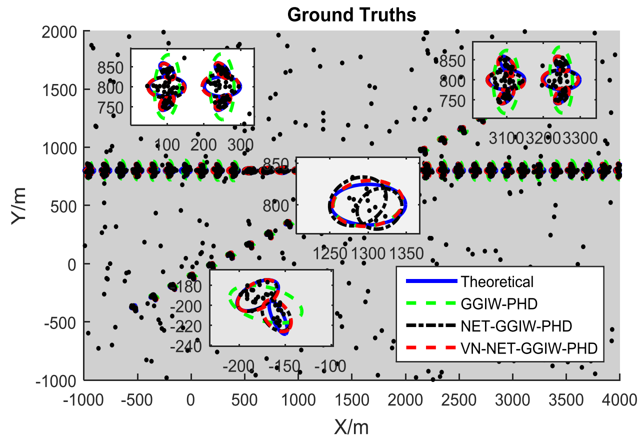

FIGURE 12. The simulation results in one trial.

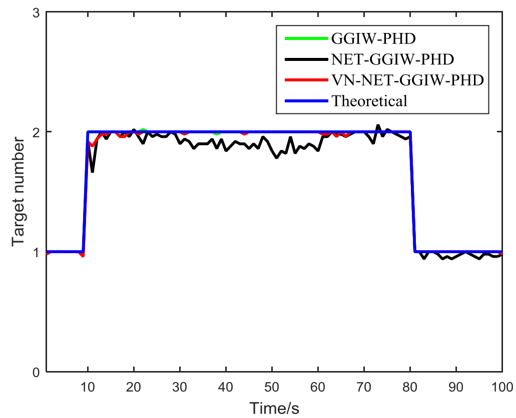

FIGURE 13. The estimate of target number.

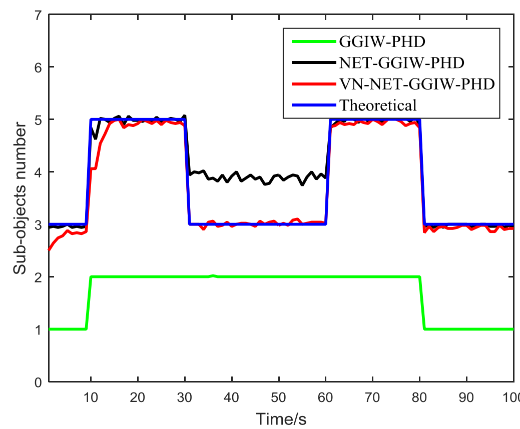

FIGURE 14. The estimate of sub-objects number.

show the estimate of target number and sub-objects number by 50 Monte Carlo trials. Similar to one target scenario, the NET-GGIW-PHD filter performs worse on the estimate of target number and sub-ellipse number when the extension state of T1 changes. The sub-objects number is nearly four instead of five due to the fact that the partition in which the group of T1 is partitioned into two cells gets a relatively larger

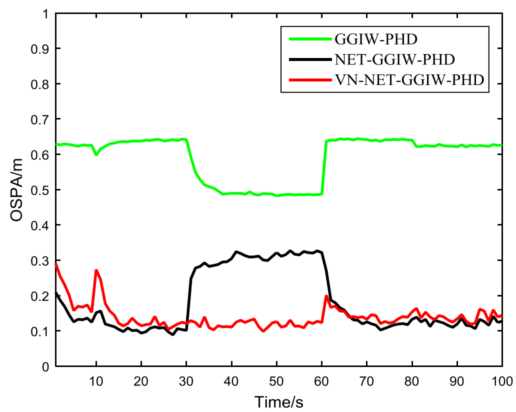

FIGURE 15. The estimate of OSPA distance.

likelihood than the partition in which the group is partitioned into three cells. And then the group of T1 is considered to be composed of two sub-objects. The GGIW-PHD filter cannot estimate the true sub-objects number. Compared with NET-GGIW-PHD filter and GGIW-PHD filter, the VN-NET-GGIW-PHD filter has better performance in terms of the estimate of target number or sub-objects number.

Fig. 15 shows the OSPA distance of three filters by 50 Monte Carlo trials. We can see that the VN-NET-GGIW-PHD filter performs well no matter whether the extension state is changed or not.

VII. CONCLUSION

This paper proposes a VN-NET-GGIW-PHD filter for multiple non-ellipsoidal extended targets tracking with varying number of sub-objects. Combined with ellipsoidal extended target model and target label management, each non-ellipsoidal extended target is regarded as a combination of multiple spatially close sub-objects and the association between the NET and corresponding sub-objects is realized. Utilizing the spawning and combination, the appropriate number of sub-objects for each non-ellipsoidal extended target can be adjusted automatically. To obtain the measurement set partition, an algorithm combined with CFSFDP algorithm and EM algorithm is proposed. Simulation results show that the proposed filter has superior performance when the extension state of the non-ellipsoidal extended target changes.

Actually, this paper proposes a framework of varying number of sub-objects for multiple non-ellipsoidal extended targets tracking, and it can be easily applied into other filters. In the future, we will incorporate the proposed approaches into more advanced filter, such as the CPHD filter, CBMeMBer filter, and GLMB filter.

REFERENCES

[1] R. P. S. Mahler, "Multitarget Bayes filtering via first-order multitarget moments," *IEEE Trans. Aerosp. Electron. Syst.*, vol. 39, no. 4, pp. 1152–1178, Oct. 2003.

[2] J. Hong Yoon, D. Y. Kim, and K.-J. Yoon, "Efficient importance sampling function design for sequential Monte Carlo PHD filter," *Signal Process.*, vol. 92, no. 9, pp. 2315–2321, Sep. 2012.

[3] R. P. S. Mahler, *Statistical Multisource-Multitarget Information Fusion*. Norwood, MA, USA: Artech House, 2007.

[4] K. Granstrom, C. Lundquist, and U. Orguner, "Tracking rectangular and elliptical extended targets using laser measurements," in *Proc. IEEE Conf. Inf. Fusion*, Jul. 2011, pp. 592–599.

[5] L. Mihaylova, A. Y. Carmi, F. Septier, A. Gning, S. K. Pang, and S. Godsill, "Overview of Bayesian sequential Monte Carlo methods for group and extended object tracking," *Digit. Signal Process.*, vol. 25, pp. 1–16, Feb. 2014, doi: 10.1016/j.dsp.2013.11.006.

[6] J. Yang, F. Liu, H. Ge, and Y. Yuan, "Multiple extended target tracking algorithm based on GM-PHD filter and spectral clustering," *EURASIP J. Adv. Signal Process.*, vol. 2014, no. 1, pp. 1–8, Dec. 2014.

[7] K. Gilholm and D. Salmond, "Spatial distribution model for tracking extended objects," *IEE Proc.-Radar, Sonar Navigat.*, vol. 152, no. 5, pp. 364–371, Oct. 2005.

[8] R. Mahler, "PHD filters for nonstandard targets, I: Extended targets," in *Proc. 12th Int. Conf. Inf. Fusion*, Jul. 2009, pp. 915–921.

[9] K. Granstrom, C. Lundquist, and O. Orguner, "Extended target tracking using a Gaussian-mixture PHD filter," *IEEE Trans. Aerosp. Electron. Syst.*, vol. 48, no. 4, pp. 3268–3286, Oct. 2012.

[10] Y. Li, H. Xiao, Z. Song, R. Hu, and H. Fan, "A new multiple extended target tracking algorithm using PHD filter," *Signal Process.*, vol. 93, no. 12, pp. 3578–3588, Dec. 2013.

[11] G. Zhang, F. Lian, and C. Han, "CBMeMBer filters for nonstandard targets, I: Extended targets," in *Proc. Int. Conf. Inf. Fusion*, Jul. 2014, pp. 1–6.

[12] U. Orguner, C. Lundquist, and K. Granstrom, "Extended target tracking with a cardinalized probability hypothesis density filter," in *Proc. IEEE Conf. Inf. Fusion*, Jul. 2011, pp. 65–72.

[13] J. W. Koch, "Bayesian approach to extended object and cluster tracking using random matrices," *IEEE Trans. Aerosp. Electron. Syst.*, vol. 44, no. 3, pp. 1042–1059, Jul. 2008.

[14] M. Feldmann, D. Franken, and W. Koch, "Tracking of extended objects and group targets using random matrices," *IEEE Trans. Signal Process.*, vol. 59, no. 4, pp. 1409–1420, Apr. 2011.

[15] K. Granstrom and U. Orguner, "A PHD filter for tracking multiple extended targets using random matrices," *IEEE Trans. Signal Process.*, vol. 60, no. 11, pp. 5657–5671, Nov. 2012.

[16] K. Granstrom, A. Natale, P. Braca, G. Ludeno, and F. Serafino, "Gamma Gaussian inverse Wishart probability hypothesis density for extended target tracking using X-band marine radar data," *IEEE Trans. Geosci. Remote Sens.*, vol. 53, no. 12, pp. 6617–6631, Dec. 2015.

[17] C. Lundquist, K. Granstrom, and U. Orguner, "An extended target CPHD filter and a gamma Gaussian inverse Wishart implementation," *IEEE J. Sel. Topics Signal Process.*, vol. 7, no. 3, pp. 472–483, Jun. 2013.

[18] M. Beard, S. Reuter, K. Granstrom, B.-T. Vo, B.-N. Vo, and A. Scheel, "Multiple extended target tracking with labeled random finite sets," *IEEE Trans. Signal Process.*, vol. 64, no. 7, pp. 1638–1653, Apr. 2016.

[19] J. Lan and X. R. Li, "Tracking of maneuvering non-ellipsoidal extended object or target group using random matrix," *IEEE Trans. Signal Process.*, vol. 62, no. 9, pp. 2450–2463, May 2014.

[20] Z. Liang, F. Liu, and J. Gao, "Improved GGIW-PHD filter for maneuvering non-ellipsoidal extended targets or group targets tracking based on sub-random matrices," *PLoS ONE*, vol. 13, no. 2, Feb. 2018, Art. no. e0192473.

[21] P. Zong and M. Barbary, "Improved multi-Bernoulli filter for extended stealth targets tracking based on sub-random matrices," *IEEE Sensors J.*, vol. 16, no. 5, pp. 1428–1447, Mar. 2016.

[22] Z. Liang, F. Liu, L. Li, and J. Gao, "Improved generalized labeled multi-Bernoulli filter for non-ellipsoidal extended targets or group targets tracking based on random sub-matrices," *Digit. Signal Process.*, vol. 99, Apr. 2020, Art. no. 102669.

[23] Q. Hu, H. Ji, and Y. Zhang, "Tracking of maneuvering non-ellipsoidal extended target with varying number of sub-objects," *Mech. Syst. Signal Process.*, vol. 99, pp. 262–284, Jan. 2018.

[24] Y. Han, H. Zhu, and C. Han, "Maintaining track continuity for extended targets using Gaussian-mixture probability hypothesis density filter," *Math. Problems Eng.*, vol. 2015, pp. 1–16, Aug. 2015.

[25] K. Granstrom and U. Orguner, "On spawning and combination of extended/group targets modeled with random matrices," *IEEE Trans. Signal Process.*, vol. 61, no. 3, pp. 678–692, Feb. 2013.

[26] Y. Zhang and H. Ji, "A novel fast partitioning algorithm for extended target tracking using a Gaussian mixture PHD filter," *Signal Process.*, vol. 93, no. 11, pp. 2975–2985, Nov. 2013.

[27] A. Rodriguez and A. Laio, "Clustering by fast search and find of density peaks," *Science*, vol. 344, no. 6191, pp. 1492–1496, Jun. 2014.
[28] A. Mukherjee and A. Sengupta, "Likelihood function modeling of particle filter in presence of non-stationary non-Gaussian measurement noise," *Signal Process.*, vol. 90, no. 6, pp. 1873–1885, Jun. 2010.
[29] X. Zhou, Y. F. Li, and B. He, "Entropy distribution and coverage rate-based birth intensity estimation in GM-PHD filter for multi-target visual tracking," *Signal Process.*, vol. 94, pp. 650–660, Jan. 2014.
[30] G. Schwarz, "Estimating dimensions of a model," *Ann. Statist.*, vol. 6, no. 2, pp. 461–464, 1978.
[31] J. Rissanen, "Modeling by shortest data description," *Automatica*, vol. 14, no. 5, pp. 465–471, Sep. 1978.
[32] H. Akaike, "A new look at the statistical model identification," *IEEE Trans. Autom. Control*, vol. AC-19, no. 6, pp. 716–723, Dec. 1974.
[33] K. Granstrom and U. Orguner, "Implementation of the GIW-PHD filter," Autom. Control, Linköping Universitet, Linköping, Sweden, Tech. Rep. LiTH-ISY-R-3046, 2012, pp. 1–9.

YANG GONG was born in Suizhou, Hubei, China, in 1992. He received the B.S. and M.S. degrees from the Institute of Electronic Engineering, Hefei, China, in 2014 and 2016, respectively. He is currently pursuing the Ph.D. degree with the College of Electronic Engineering, National University of Defense Technology. His research interests include target tracking and adaptive signal processing.

CHEN CUI was born in Yixian, Hebei, China, in 1962. He received the B.S. degree from the Institute of Electronic Engineering, Hefei, China, in 1984, and the M.S. degree from the University of Science and Technology of China, in 1991. He is currently a Professor with the College of Electronic Engineering, National University of Defense Technology. His research interests include adaptive signal processing, radar waveform design, and the signal processing in electronic countermeasures.

BIAO WU was born in Bozhou, Anhui, China, in 1991. He received the B.S. and M.S. degrees from the Institute of Electronic Engineering, Hefei, China, in 2013 and 2016, respectively. He is currently working with the Huayin Ordnance Test Center. His research interests include target tracking and adaptive signal processing.